Benchmarks of breakup models

Prog. Part. Nucl. Phys. 101 (2018) 154, Phys. Scr. T152 (2013) 014019

Jin Lei and AB, in preparation

Angela Bonaccorso

INFN
Sezione di Pisa

https://reactionseminar.github.io/
30th April 2020

Plan of the Presentation

Transfer to continuum states (inclusive reaction)

Kinematics and phase space ++

Single particle state properties (shell model)

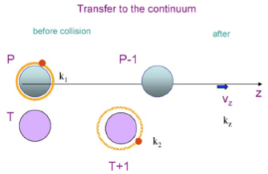

$k_2 - k_1 = k_z$

$\varepsilon_f - \varepsilon_i = mv^2/2$

Fragmentation reaction (coincidence)

Let us start with a two neutron halo nucleus like ^{11}Li or ^{14}Be

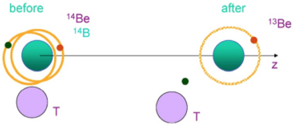

Coulomb breakup (inclusive or coincidence)

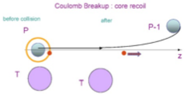

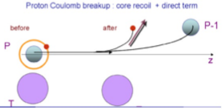

Examples of reactions

TC: n+target interaction

- T(d,p)T+n$\rightarrow$ *surrogate*, *TrojanHorse*
- ^{9}Li(d,p)^{10}Li$\rightarrow$ *Mario Gomez*
- ^{9}Be(^{18}O,^{17}O)^{10}Be
- ^{9}Be(^{18}O,^{16}O)^{11}Be
- ^{9}Be(^{14}O,^{13}O)X(^{9}Be+n)

Fragmentation: n+core interaction

- ^{11}Li(^{12}C,X)^{9}Li+n $\rightarrow$ *A.Corsi*, *M.Gomez*
- ^{14}Be(^{12}C,X)^{12}Be+n $\rightarrow$ *A.C.*
-
-
-

Structure study motivation for exotic nuclei at the drip line and beyond (unbound).

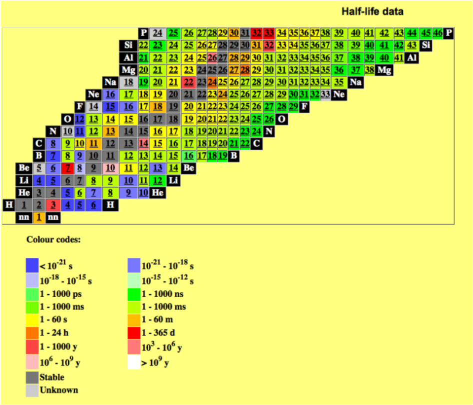

- Check the limits of validity of structure models such as the SHELL MODEL or "ab initio" models, understanding of the *residual* nuclear force.
- Challenges in breakup reaction theories.

For normal nuclei: study of low lying resonance properties and/or damping of high L single particle states in the continuum.

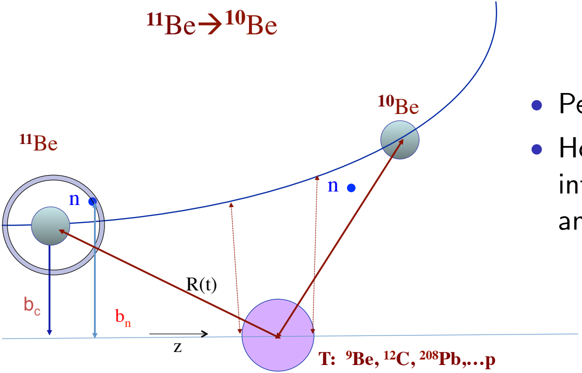

- Peripheral reaction
- How important is the internal part of the initial and final n wave function

Theoretical models for inclusive (nonelastic) breakup [20]

- Requires inclusion of all possible processes through which the breakup fragment can interact with the target. Impractical in most cases.

In 1980s

- Ichimura, Austern, and Vincent developed a spectator-participant model (post-form) — Phys. Rev. *C* 23, 1847 (1981); Phys. Rev. *C* 32, 431 (1985)
- Udagawa and Tamura suggested a breakup-fusion model (prior-form) — Phys. Rev. *C* 24, 1348 (1981); Phys. Lett. B 135, 333(1984)
- Hussein and McVoy adopted a spectator model with the Feshbach projection method — Nucl. Phys. *A* 445, 124 (1985)
- Three different approaches with different predictions

Goals

- Find a suitable model for inclusive breakup
- Explore relations between these models

Challenges

- Numerically difficult
- No numerical implementation in 1980s-2000s even for Finite Range DWBA

Semiclassical methods proposed: W. Baur et al., D.M. Brink and A.B.

The Ichimura, Austern, Vincent (IAV) model

- Inclusive breakup :
  - a + A ⟶ b + anything ⟶ (x+A)*

    b+x

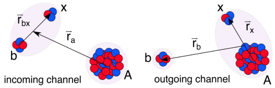

Any possible states between x and A (including all nucleons degree of freedom)

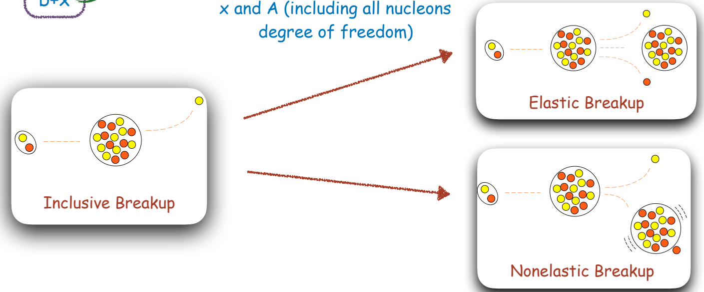

- Project all degrees of freedom into three body model space

$$\left.\frac{d^2\sigma}{dE_b d\Omega_b}\right|_{NEB} = -\frac{2}{\hbar v_a}\rho_b(E_b)\langle \varphi_x(\vec{k}_b)|W_x|\varphi_x(\vec{k}_b)\rangle$$

Imaginary part of x-A effective interaction

Jin Lei and A. M. Moro, PRC.92.044616, PRL 123, 232501 (2019); cf. Eq. (2.21) of IAV

$$\left.\frac{d^2\sigma}{dE_b d\Omega_b}\right|_{\mathrm{NEB}} = -\frac{2}{\hbar v_a}\rho_b(E_b)\langle\varphi_x(\mathbf{k}_b)|\mathrm{Im}[U_{xA}]|\varphi_x(\mathbf{k}_b)\rangle, \tag{3}$$

where $\rho_b(E_b)$ is the density of states of the particle b, v_a is the velocity of the incoming particle, U_{xA} is the optical potential describing $x+A$ elastic scattering, and $\varphi_x(\mathbf{k}_b, \mathbf{r}_{xA})$ is a relative wave function describing the motion between x and A when particle b is scattered with momentum $\mathbf{k}_b$. This function is obtained from the equation

$$\varphi_x(\mathbf{k}_b, \mathbf{r}_x) = \int G_x(\mathbf{r}_x, \mathbf{r}'_x)\langle \mathbf{r}'_x \chi_b^{(-)}|V_{\mathrm{post}}|\Psi^{3b(+)}\rangle d\mathbf{r}'_x \tag{4}$$

where G_x is the Green's function with optical potential U_{xA}, $\chi_b^{(-)*}(\mathbf{k}_b, \mathbf{r}_b)$ is the distorted wave describing the relative motion between b and B^* compound system (obtained with some optical potential U_{bB}), $V_{\mathrm{post}} \equiv V_{bx} + U_{bA} - U_{bB}$ is the postform transition operator and $\Psi^{3b(+)}$ the three-body scattering wave function. Note that the imaginary part of U_{xA} accounts for all nonelastic processes between x and A and hence Eq. (3) includes the ICF as well as other NEB contributions. Further details can be found in Ref. [31] and in the Supplemental Material, Sec. II [42].

A consistent formalism for all breakup reaction mechanisms

The core-target movement is treated in a semiclassical way, but neutron-target and/or neutron-core with a full QM method.

AB and DM Brink, PRC38, 1776 (1988), PRC43, 299 (1991), PRC44, 1559 (1991).

Early eikonal model: I. Tanihata, Prog. Part. Nucl. Phys. 35, 505 (1995), halo-core decoupling.

$$\frac{d\sigma}{d\xi} = C^2 S \int_0^\infty d\mathbf{b_c} \frac{dP_{-n}(b_c)}{d\xi} P_{ct}(b_c),$$

$\otimes$

$$\xi \to \varepsilon_f, k_z, P_{//} \quad also \quad ANC = \sqrt{C^2 S C_i^2}$$

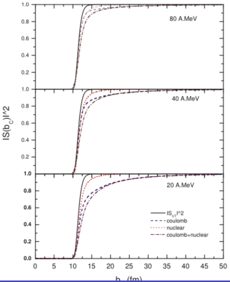

Use of the simple parametrization

$$P_{ct}(b_c) = |S_{ct}|^2 = e^{(-\ln 2 exp[(R_s - b_c)/a])},$$

$$R_s \approx r_s(A_p^{1/3} + A_t^{1/3}) \qquad r_s \approx 1.4fm$$

'strong absorption radius'

Transfer to the continuum: from resonances to knockout reactions

First order time dependent perturbation theory amplitude: ∗∗

$$A_{fi} = \frac{1}{i\hbar}\int_{-\infty}^{\infty} dt < \phi_f(\mathbf{r})|V(\mathbf{r})|\phi_i(\mathbf{r}-\mathbf{R}(t)) > e^{-i(\omega t - mvz/\hbar)} \qquad (1)$$

$$\omega = \varepsilon_i - \varepsilon_f + \tfrac{1}{2}mv^2 \qquad \mathbf{R}(t) = \mathbf{b_c} + vt$$

$$\begin{aligned}\frac{dP_{-n}(b_c)}{d\varepsilon_f} &= \frac{1}{8\pi^3}\frac{m}{\hbar^2 k_f}\frac{1}{2l_i+1}\Sigma_{m_i}|A_{fi}|^2 \\ &\approx \frac{4\pi}{2k_f^2}\Sigma_{j_f}(2j_f+1)(|1-\bar{S}_{j_f}|^2 + 1 - |\bar{S}_{j_f}|^2)\mathcal{F},\end{aligned}$$

ϕ_f see (∗)

$$\mathcal{F} = (1 + F_{l_f,l_i,j_f,j_i})B_{l_f,l_i} \qquad B_{l_f,l_i} = \frac{1}{4\pi}\left[\frac{k_f}{mv^2}\right]|C_i|^2\frac{e^{-2\eta b_c}}{2\eta b_c}M_{l_f l_i}$$

Neutron wave functions

Final continuum state:

$$\phi_{l_f}(\mathbf{r}) = C_f k \frac{i}{2}\left(h_{l_f}^{(+)}(kr) - \bar{S}_{l_f} h_{l_f}^{(-)}(kr)\right) Y_{l_f,m_f}(\Omega_f),$$

$\bar{S}_{l_f}(\varepsilon_f)$ is an optical model (n-core in fragmentation reactions, n-target in knockout reactions) S-matrix.

Initial state:

$$\phi_{l_i}(\mathbf{r}) = -C_i i^l \gamma h_{l_i}^{(1)}(i\gamma r) Y_{l_i,m_i}(\Omega_i).$$

Surface approximation: G. Baur & Co., NPA311 (1978) 141,PRC.28, 946, PR111(1984)333; A. Winter & Co., L. Lo Monaco and D.M. Brink JPG11, 935, 1985; A. Mukhamedzhanov PRC 84, 044616, 2011; I. Thomposon talk at DREB2012 (Pisa).

Eikonal limit

Small neutron scattering angles

$$M_{l_f l_i} \approx P_{l_i}(X_i) P_{l_f}(X_f); \qquad P_{l_f}(X_f) \to I_0(2\eta \mathbf{b_v})$$

large n-t angular momenta

$$\frac{4\pi}{2k_f^2} \Sigma_{j_f}(2j_f + 1) \to \int_0^\infty d\mathbf{b_v}$$

both conditions might not be well satisfied for stripping of deeply bound nucleons unless the core-target scattering is very peripheral. Verify core angular distributions.

$$P_{-n}(\mathbf{b_c}) = \int_0^\infty d\mathbf{b_v}(|1 - \bar{S}(b_v)|^2 + 1 - |\bar{S}(b_v)|^2)|\tilde{\phi}_i(|\mathbf{b_v} - \mathbf{b_c}|, k_1)|^2$$

Notice $k_1 \to -\infty$ not strictly necessary.

$^{14}O(^{9}Be,X)^{13}O$

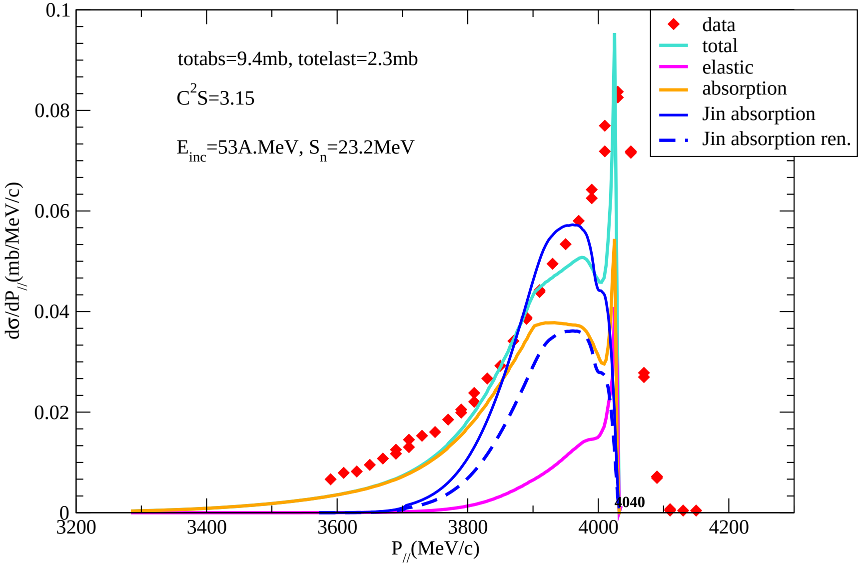
totabs=9.4mb, totelast=2.3mb
C^2S=3.15
E_{inc}=53A.MeV, S_n=23.2MeV
data
total
elastic
absorption
Jin absorption
Jin absorption ren.
4040
$d\sigma/dP_{//}$(mb/MeV/c)
$P_{//}$(MeV/c)
0
0.02
0.04
0.06
0.08
0.1
3200
3400
3600
3800
4000
4200

Example "deformation" effects due to n-target interaction and kinematical cut-off.

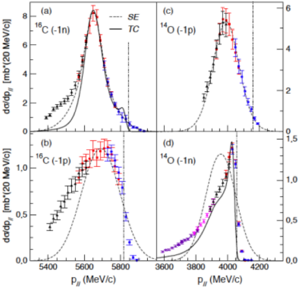

F. Flavigny, A. Obertelli, AB et al.
PRL 108, 252501 (2012).

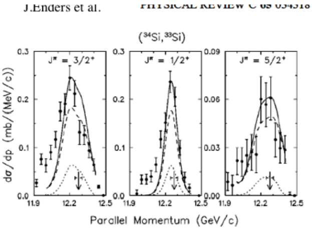

J.Enders et al. PRC65.034318

Asymmetries at high incident energy

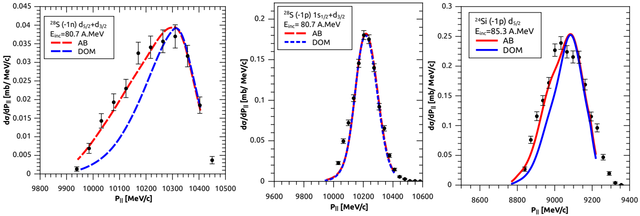

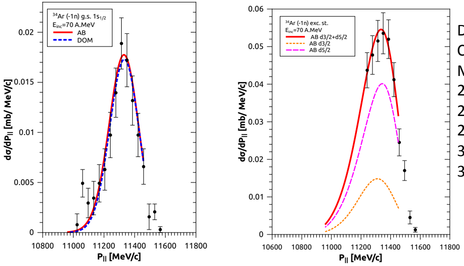

Data courtesy of A. Gade
Calculations G. Salvioni
MSc Thesis in preparation.
28S (-1n) 80.7 d5/2+d3/2
28S (-1p) s1/2+d3/2 A.MeV
24Si(-1p) d5/2 85.3 A.MeV
34Ar (-1n) s1/2 gs 70 A.MeV
34Ar (-1n) d3/2+d5/2

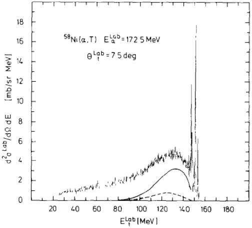

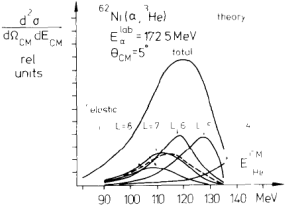

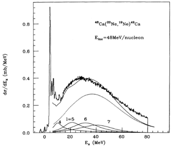

FIG. 7. Results of the reaction ^{48}Ca(^{20}Ne,^{19}Ne)^{49}Ca at E_{inc} = 48 MeV/nucleon [8]. The solid curve superimposed onto the experimental spectrum is the calculated inclusive cross section. The dotted curve is the total breakup. The final angular momentum decomposition is shown in the lower part of the figure.

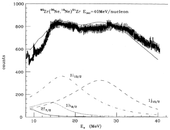

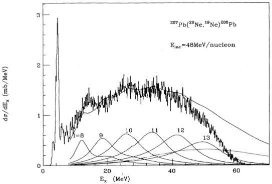

M. Hussein, Mc Voy. NPA445(1985)124

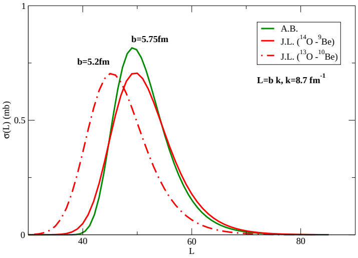

M.S. Hussein, K.W. McVoy / Inclusive projectile fragmentation

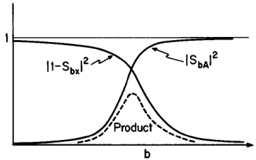

Fig. 2. Schematic representation of the absorption factors of eq. (4.17), indicating how they integration to the surface region of the target.

sees from eqs. (4.9) and (4.12) that the total yield of fragment b is

$$Y_b \equiv \int \frac{d^2\sigma_R}{d\Omega_b \, dE_b} d^3q = \frac{2}{v_a}(2\pi)^3 \frac{E_x}{\hbar k_x} \int d^3r_b \, d^3r_x$$
$$\times |S_{bA}(b_b)|^2 |\phi_a(\boldsymbol{r}_b - \boldsymbol{r}_x)|^2 \left[1 - |S_{xA}(b_x)|^2\right].$$

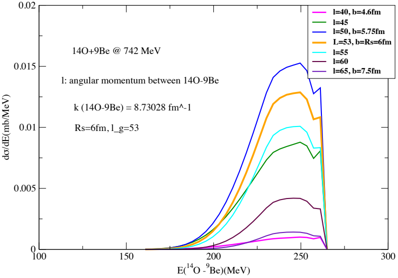
14O+9Be @ 742 MeV
l: angular momentum between 14O-9Be
k (14O-9Be) = 8.73028 fm^-1
Rs=6fm, l_g=53
l=40, b=4.6fm
l=45
l=50, b=5.75fm
L=53, b=Rs=6fm
l=55
l=60
l=65, b=7.5fm
dσ/dE(mb/MeV)
E(^{14}O - ^{9}Be)(MeV)

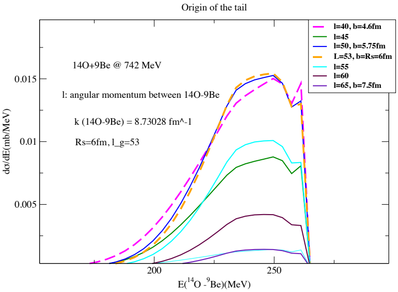
Origin of the tail
14O+9Be @ 742 MeV
l: angular momentum between 14O-9Be
k (14O-9Be) = 8.73028 fm^-1
Rs=6fm, l_g=53
l=40, b=4.6fm
l=45
l=50, b=5.75fm
L=53, b=Rs=6fm
l=55
l=60
l=65, b=7.5fm
dσ/dE(mb/MeV)
E(^{14}O - ^{9}Be)(MeV)

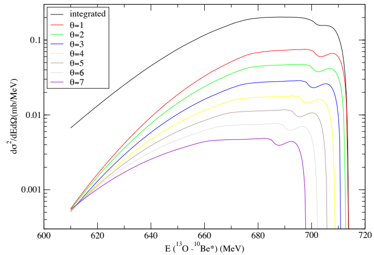
integrated
θ=1
θ=2
θ=3
θ=4
θ=5
θ=6
θ=7
dσ^2/dEdΩ(mb/MeV)
E (^{13}O - ^{10}Be*) (MeV)

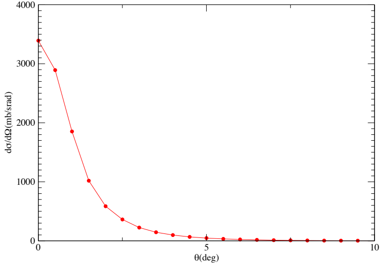
dσ/dΩ(mb/srad)
θ(deg)

Initial wave function

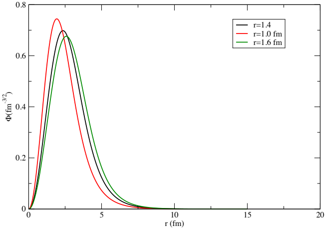

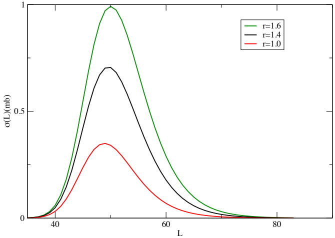

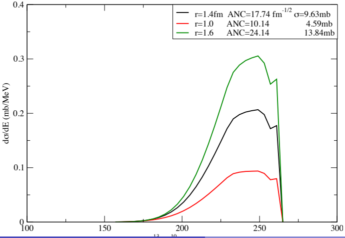

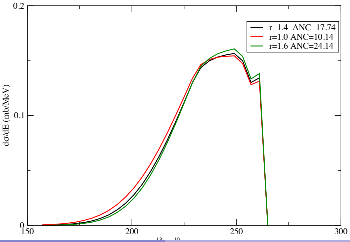

n-^{9}Be optical potential: A.B & R.J. Charity, PRC89, 024619 (2014)

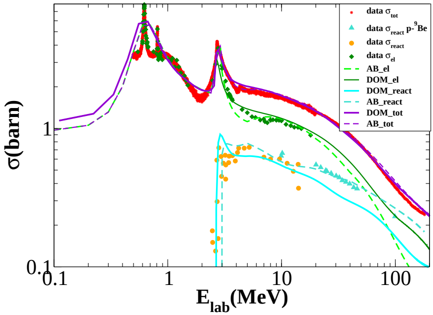

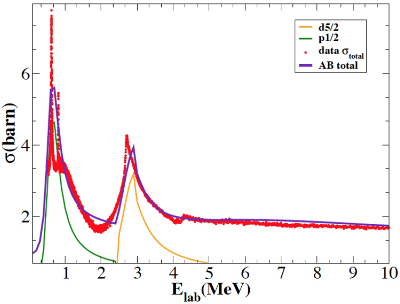

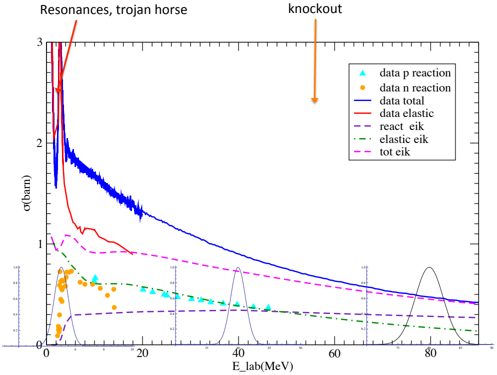
Resonances, trojan horse
knockout
data p reaction
data n reaction
data total
data elastic
react eik
elastic eik
tot eik
σ(barn)
E_lab(MeV)
0
1
2
3
0
20
40
60
80

Transfer to ^{10}Be, ^{11}Be resonances: missing mass experiment.

Phys. Rev. C90, 064621 (2014), Phys. Rev. C100, 024617 (2019).

Diana Carbone, AB, Mariangela Bondì, F. Cappuzzello, M Cavallaro et al. MAGNEX Collaboration:
1n and 2n transfer experimental campaign

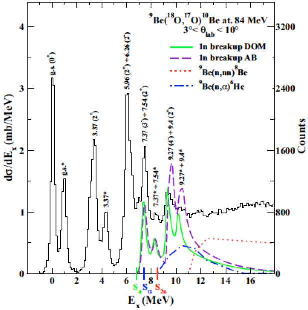

^{16} O has a degenerate gs (1d5/2,2s1/2)
^{17} O has 5/2+ gs and 1/2+ first excited state at E*=0.87MeV

Position and widths of p1/2 and d5/2 resonances in ^{10}Be perfectly reproduced

d5/2 resonance in ^{11}Be perfectly reproduced
Evidence for a ^{10}Be (2+)+n(d5/2) at Ex=5.8MeV

n-10Be Smatrix from
A. Calci et al., PRL**117**.242501

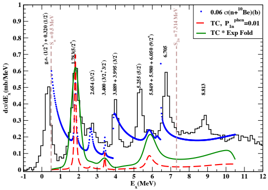

A.B, D. Carbone, F. Cappuzzello, M Cavallaro, G. Hupin, P. Navrátil, and S. Quaglioni

Based on A. Calci et al., PRL

Single folding vs double folding

A target used very often is ^{9}Be
→ single folding of a n-^{9}Be phenomenological potential with a microscopic projectile density

PHYSICAL REVIEW C **94**, 034604 (2016)

Imaginary part of the ^{9}C-^{9}Be single-folded optical potential

A. Bonaccorso,[1,*] F. Carstoiu,[2] and R. J. Charity[3]

Few-Body Syst (2016) 57:331–336
DOI 10.1007/s00601-016-1082-4

**A. Bonaccorso · F. Carstoiu · R. J. Charity · R. Kumar
G. Salvioni**

Differences Between a Single- and a Double-Folding Nucleus-^{9}Be Optical Potential

The Glauber reaction cross section is given by

$$\sigma_R = 2\pi \int_0^\infty b\, db(1 - |S_{NN}(\mathbf{b})|^2) \tag{1}$$

where

$$|S_{NN}(\mathbf{b})|^2 = e^{2\chi_I(b)} \tag{2}$$

is the probability that the nucleus-nucleus (NN) scattering is elastic for a given impact parameter **b**.

The imaginary part of the eikonal phase shift is given by

$$\chi_I(\mathbf{b}) = \frac{1}{\hbar v}\int dz\, W^{NN}(\mathbf{b}, z) = \frac{1}{\hbar v}\int dz \int d\mathbf{r_1} W^{nN}(\mathbf{r_1} - \mathbf{r})\rho(\mathbf{r_1}) \tag{3}$$

where W^{NN} is negative defined as

$$W^{NN}(\mathbf{r}) = \int d\mathbf{b_1} W^{nN}(\mathbf{b_1} - \mathbf{b}, z) \int dz_1\, \rho(\mathbf{b_1}, z_1). \tag{4}$$

In the double-folding method, W^{NN} is obtained from the microscopic densities $\rho_{p,t}(\mathbf{r})$ for the projectile and target respectively and an energy-dependent nucleon-nucleon (nn) cross section σ_{nn}, i.e.,

$$W^{NN}(\mathbf{r}) = -\frac{1}{2}\hbar v \sigma_{nn} \int d\mathbf{b_1}\, \rho_p(\mathbf{b_1} - \mathbf{b}, z) \int dz_1\, \rho_t(\mathbf{b_1}, z_1). \tag{5}$$

Also

$$W^{nN}(\mathbf{r}) = -\frac{1}{2}\hbar v \sigma_{nn} \rho_t(\mathbf{r}) \tag{6}$$

is a single-folded zero-range n-target imaginary potential and v is the nucleon-target velocity of relative motion. The W^{nN} potential of Eq.(6) has the same range as the target density because σ_{nn} is a simple scaling factor.

8Li and 8B data from

8. G. W. Fan et al., Phys. Rev. C90 (2014) 044321.
9. M. Fukuda et al., Nucl. Phys. A656 (1999) 209.

9C data from Fukuda, Nishimura, private communication

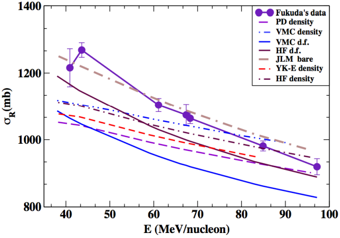

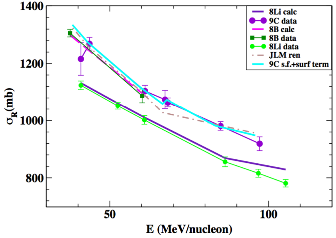

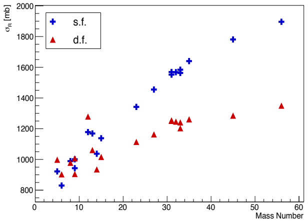

Imane Moumene,AB in preparation

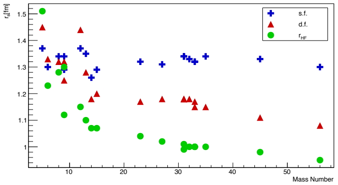

Kinematics

From Eq.1 ** by the change of variables $dtdxdydz \rightarrow dxdydzdz'$
$e^{-i(\omega t - mvz/\hbar)} \rightarrow e^{-ik_1 z'} e^{ik_2 z}$ neutron energies to neutron parallel momenta with respect to core

$$k_1 = \frac{\varepsilon_f - \varepsilon_i - \frac{1}{2}mv^2}{\hbar v};$$

to target

$$k_2 = \frac{\varepsilon_f - \varepsilon_i + \frac{1}{2}mv^2}{\hbar v};$$

to core parallel momentum

$$\begin{aligned} P_{//} &= \sqrt{E_r^2 - M_r^2} = \sqrt{(T_r + M_r)^2 - M_r^2} \\ &= \sqrt{(T_p + \varepsilon_i - \varepsilon_f)^2 + 2M_r(T_p + \varepsilon_i - \varepsilon_f)}, \end{aligned} \qquad (2)$$

breakup threshold at $\varepsilon_f = 0$
++**

Exact 4-vec conservation, see https://arxiv.org/ftp/arxiv/papers/1011/1011.1943.pdf

Origin of kinematical cut-off (phase space) and deformation effects

PRC60(1999) 054604,PRC44(1991) 1559,AB and GF Bertsch, PRC63(2001) 044604, F. Flavigny, A. Obertelli, AB et al., PRL 108, 252501 (2012). $(+)$

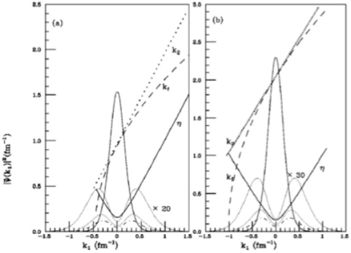

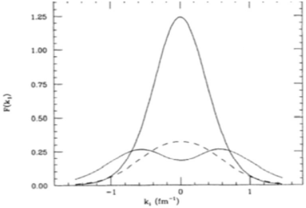

FIG. 11. Initial-state momentum distributions in ^{20}Ne according to Eq. (2.3a). The solid curve is for the $2s_{1/2}$ state, the dashed curve is the for $1p_{1/2}$, while the dotted curve is for the

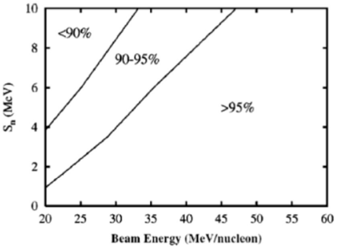

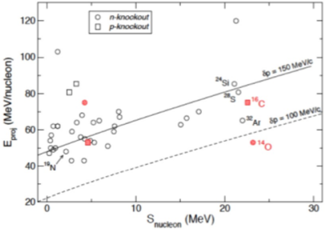

$^{12}Be(^{9}Be,X)^{11}Be$@78A.MeV

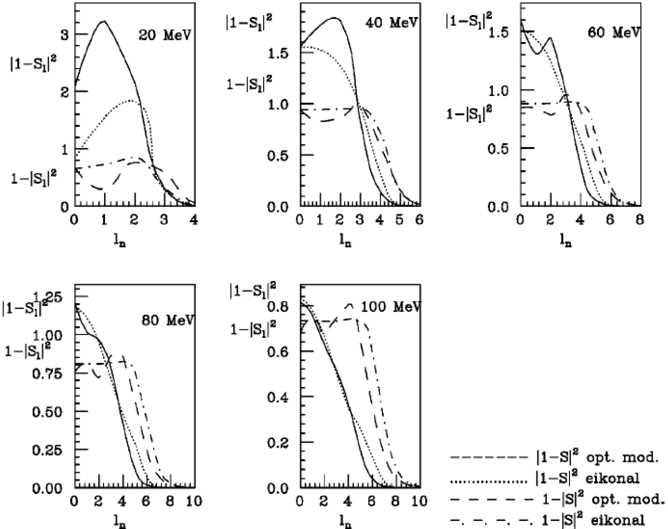

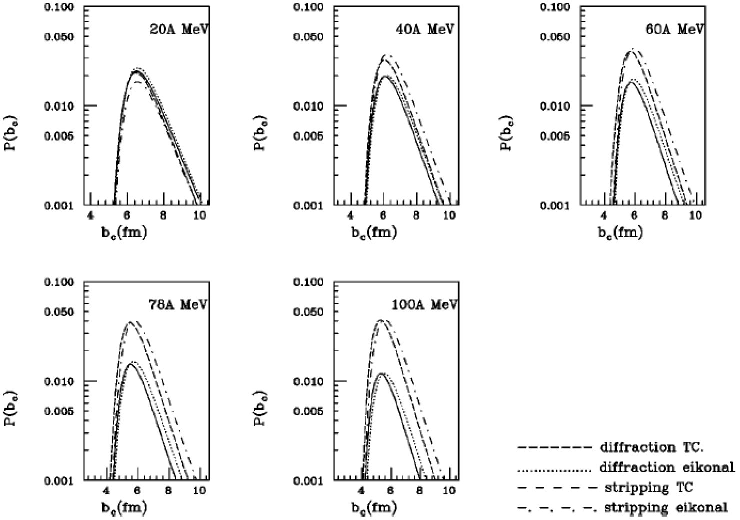
20A MeV
40A MeV
60A MeV
78A MeV
100A MeV
P(b$_c$)
b$_c$(fm)
0.100
0.050
0.010
0.005
0.001
4
6
8
10
diffraction TC.
diffraction eikonal
stripping TC
stripping eikonal

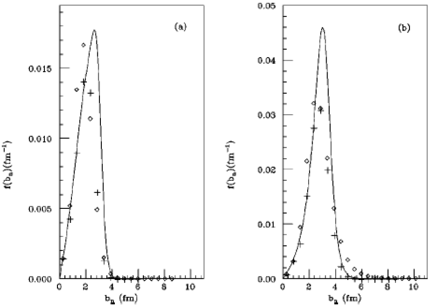

FIG. 5. The integrand function of the diffraction (a), and stripping (b) term of Eq. (11) after k_z integration, full curve, obtained from the realistic bound state wave function and the corresponding terms, diamonds, in the sum over partial waves of Eqs. (5) and (6) in the case of the incident energy of 78*A* MeV. Crosses are the results of a calculation of Eq. (11) in which the eikonal phase shifts have been substituted by the optical model phase shifts as in Eq. (B9). All calculations done at fixed impact parameter $b_c = 5.6$ fm between the projectile and target.

^{13}Be puzzle or of the "elusive 1/2+ state in Be isotopes

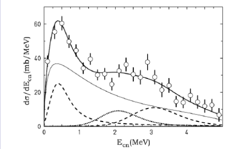

Figure : (a) GSI, H. Simon et al. NPA791 (2007) 267.

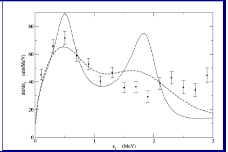

Figure : (b) G.Blanchon et al. NPA784 (2007) 49.

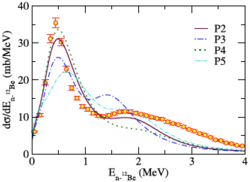

A. Corsi et al., PLB.797.1344843

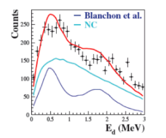

(b) G. Randisi, N. Orr et al. Phys. Rev. C 89, 034320

$$(d\delta_l/d\varepsilon)_{res} = 2/\Gamma_j$$

Energies and widths of unbound p- and d-states in ^{13}Be and corresponding strength parameters for the δV potential

	ε_{res} (MeV)	Γ_j (MeV)	α (MeV)
$1p_{1/2}$	0.67	0.28	8.34
$1d_{5/2}$	2.0	0.40	−2.36

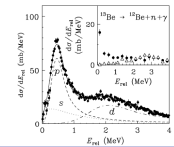

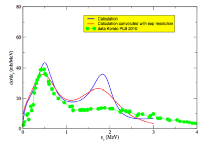

Figure : (b) RIKEN, Y. Kondo et al. PLB690 (2010) 245; G. Blanchon, private

G. Blanchon et al.
PRC82, 034313
NPA A 784 (2007) 49

Our level sequence
2s1/2 a_s=-0.8fm
1p1/2
1d5/2

- QM TC numerically challenging at high energy (large n of partial waves) and for small separation energies (DWBA source term), all observables. Semiclassical TC has a large range of validity, numerically easy, accurate. NO core angular distributions. Eikonal valid from $\approx$ 80A.MeV, only momentum distributions and total cross sections for knockout.
- Inclusive breakup reactions are dominated by final state interaction with the target at small incident energy: used as surrogate reaction
- At intermediate incident energy: strong interplay between projectile and target characteristics: "deformed' momentum distributions and cutoff effects.
- From the valence particle projectile momentum distribution at high incident energy: information on angular momentum of the initial state and possible dynamical core-target excitations.
- Coincidence experiments of breakup particle experiments (using invariant mass method) are more INdependent on incident energy (i.e.^{13}Be) case.
- Elastic scattering experiments and or total reaction cross section measurements: they can tell us about the typical interaction distances and help fixing the optical potentials.

Some of my co-authors and collaborators in historical order.

D. M. Brink
N. Vinh Mau
G. Blanchon
F. Carstoiu
G. F. Bertsch
Ravinder Kumar
F. Flavigny, A. Obertelli
R. J. Charity
MAGNEX collaboration at INFN-LNS: F. Cappuzzello, D. Carbone, M. Cavallaro,G. Hupin, P. Navratil, S. Quaglioni
G. Salvioni... see his talk at DREB2014 in Darmstadt and Master Thesis
Jin Lei.